

Research Article

Kozo Shinoda*, Seishi Abe, Kazumasa Sugiyama, and Yoshio Waseda

The local structure around Ge atoms in Ge-doped magnetite thin films

<https://doi.org/10.1515/htmp-2020-0099>

received June 15, 2020; accepted November 06, 2020

Abstract: Distribution of Ge atoms between tetrahedral and octahedral sites in the spinel-type structure of $\text{Fe}_{2.64}\text{Ge}_{0.36}\text{O}_4$ thin films fabricated by radio frequency sputtering with a composite target of magnetite and Ge has been investigated by extended X-ray absorption fine structure analysis. The local structural changes around the Ge atoms in the films induced by annealing at 573 and 873 K are discussed through comparison of the local structure for sintered crystalline $\text{Fe}_{2.7}\text{Ge}_{0.3}\text{O}_4$ in which Ge atoms preferentially located at the tetrahedral site of the spinel-type structure. This work provides successful information on the structural change with magnetic property of the thin films as follows: the Ge atoms statistically distributed at the tetrahedral and octahedral sites of the as-synthesized films and preferentially occupied the tetrahedral site by annealing at 873 K corresponding to the increase in magnetization.

Keywords: site distribution, spinel-type structure, X-ray absorption spectroscopy, single crystal X-ray diffraction

1 Introduction

Magnetite thin films have attracted much attention as devices exhibiting magnetic properties [1–3]. The properties have been investigated for the magnetite thin films synthesized by deposition methods such as molecular-beam epitaxy [4,5], dc magnetron reactive sputtering using an Fe target in Ar–O₂ gas mixture [6], and the

pulsed-laser deposition using a magnetite target [7]. Among those interesting methods, the radio frequency (RF) sputtering method using composite targets is a promising method to easily obtain a film with stoichiometric magnetite film. As an example, magnetite thin films have been produced by the RF sputtering method using composite target of Fe_3O_4 with 50% of Fe_2O_3 [8] or Fe_3O_4 with 5% of FeO [9]. In these cases, the target composition was intentionally deviated from the stoichiometry of magnetite toward oxygen excess or iron excess region to obtain the single-phase stoichiometric magnetite. On the contrary, thin films of magnetite prepared with a magnetite and Ge metal composite target exhibited superior magnetization properties [10], together with excellent resistance to oxidation, in particular ref. [11,12]. These interesting results prompted us to study the local structure around Ge atoms introduced in the magnetite thin films.

Magnetite (Fe_3O_4) has the spinel-type structure expressed by the general structure formula of AB_2O_4 with eight formula units in a cubic unit cell. A and B cations are located at the special positions 8a (A site) and 16d (B site) of the space group $Fd\bar{3}m$. One-eighth of the tetrahedral and half of the octahedral interstices of the cubic-close packed oxide anions (32e) are the A and B sites, respectively. The cations at the A and B sites are coordinated by four and six oxide anions, respectively, with different A–O and B–O interatomic distances. In the case of magnetite, Fe^{2+} cations usually prefer to occupy the octahedral B sites, and the structure is classified as an “inverse” spinel type. The structural differences are useful to determine the distribution of cations to the two sites. In this study, we investigate the local structure around the Ge atoms to clarify Ge atom distribution at the A and B sites in the magnetite thin film.

2 Experimental

2.1 Sample preparation

A thin film sample of Ge-doped magnetite was deposited on an alkali-free borosilicate glass (Corning #7059)

* Corresponding author: Kozo Shinoda, Institute of Multidisciplinary Research for Advanced Materials, Tohoku University, Sendai 980-8577, Japan, e-mail: kozo.shinoda.e8@tohoku.ac.jp

Seishi Abe: Research Institute for Electromagnetic Materials, Tomiya, Miyagi 981-3341, Japan

Kazumasa Sugiyama: Institute for Materials Research, Tohoku University, Sendai 980-8577, Japan

Yoshio Waseda: Research Institute for Electromagnetic Materials, Tomiya, Miyagi 981-3341, Japan

substrate by the RF sputtering method using a composite target of 4-in.-diameter magnetite and $5 \times 5 \text{ mm}^2$ Ge metal under 2.0×10^{-3} Torr Ar gas atmosphere for 60 min in deposition time [10]. The obtained thin film sample was subsequently annealed at 573 or 873 K in vacuum for 1 h. X-ray diffraction measurements at a fixed incident angle of 3° were performed for the annealed thin film samples using X-ray diffractometer (Rigaku RINT-2200) with Cu K α radiation. The chemical composition of the thin films was analyzed by energy dispersive spectroscopy (EDS; EDAX Phoenix).

A bulk sample of $\text{Fe}_{2.7}\text{Ge}_{0.3}\text{O}_4$ used for reference was prepared as follows. Appropriate amounts of chemical reagents FeO (99%), Fe_3O_4 (99.9%), and GeO_2 (99.999%) (Furuuchi Chemical Co., Ltd) were mixed in an agate mortar with a pestle. The powder mixture was shaped in a cylindrical pellet and subsequently heated at 1,273 K in vacuum condition for 48 h. The obtained bulk sample was crushed, and a single crystal particle of 10 μm in diameter was taken for crystal structure analysis by single crystal X-ray diffraction.

2.2 Single crystal X-ray diffraction

Single crystal X-ray data were collected using a Rigaku XtaLAB Synergy-S diffractometer equipped with a HyPix-6000HE Hybrid Photon Counting detector and Mo micro-focus sealed X-ray source. The data collection strategy was calculated within CrysAlis Pro (Rigaku OD, 2018) [13] to ensure desired data redundancy and completeness. Scattering factors for neutral atoms and anomalous dispersion coefficients were taken from International Tables for Crystallography Volume C (1992) [14]. The least-squares refinement was carried out using the software program SHELXL (Sheldrick, 2008) [15]. Crystal data and structural refinement details are summarized in Table 1.

2.3 X-ray absorption spectroscopy

The local structures around the Ge atoms for the film samples and the reference $\text{Fe}_{2.7}\text{Ge}_{0.3}\text{O}_4$ bulk sample were characterized by X-ray absorption spectroscopy (XAS). Measurements of X-ray absorption spectra in X-ray absorption near edge structure (XANES) and extended X-ray absorption fine structure (EXAFS) regions around Ge K absorption edge ($11,103 \text{ eV} = 1.7789 \times 10^{-15} \text{ J}$) in a

Table 1: Experimental details of single crystal X-ray diffraction measurement

Chemical formula	$\text{Fe}_{2.7}\text{Ge}_{0.3}\text{O}_4$
Crystal system, space group	cubic, $Fd\bar{3}m$
a (nm)	0.84049(2)
V (nm^3)	0.59375(5)
Z	8
Radiation type, wave length (nm)	Mo K α , 0.071073
μ (mm^{-1})	15.854
Crystal size (mm)	$0.31 \times 0.27 \times 0.26$
Diffractometer	Rigaku XtaL AB Synergy
Absorption correction	Gaussian
$T_{\text{min.}}, T_{\text{max.}}$	0.741, 0.783
No. of measured, independent, and observed [$I > 2\sigma(I)$] reflections	1131, 190, 149
$R_{\text{int.}}, R_{\text{equ.}}$	0.0102, 0.0136
$\theta_{\text{min.}}, \theta_{\text{max.}}$ (deg.)	4.200, 51.120
$R[F^2 > 2\sigma(F^2)], wR(F^2), S$	0.0106, 0.0287, 1.161
No. of parameters	10
$\Delta\rho_{\text{max.}}, \Delta\rho_{\text{min.}}$ (10^{-3} e nm)	0.33, -0.55

fluorescence-yield mode were carried out using laboratory X-ray absorption spectrometer (R-XAS Looper; Rigaku Co., Ltd) [16]. White X-ray emitted from an unsealed X-ray tube with a Mo target and LaB $_6$ filament was monochromized using a Johansson-type bent monochromator with Si 620 for XANES and Si 400 for EXAFS measurements. The monochromized X-ray was irradiated on the sample pass through an Ar gas-sealed proportional counter as an intensity monitor for incident X-ray. The Fe and Ge K α fluorescence and elastic scattering X-rays emitted from the sample were detected with a silicon drift detector (XSDD50-01Be; TechnoAP Co. Ltd). The Ge K α fluorescence was electrically filtered by a digital spectrometer (APU101X; TechnoAP Co. Ltd). The collected XAFS spectra were characterized using the Demeter package [17] including software Athena for data processing and Artemis for determination of structure parameters with FEFF 6 code [18].

3 Results and discussion

3.1 Thin film formation

Figure 1 shows the X-ray diffraction patterns of the as-synthesized and annealed thin film samples. These pattern profiles indicated that all thin film samples consist only of crystalline phase of the spinel structure. The

atomic ratio of Fe:Ge analyzed by EDS was 0.88:0.12. Considering that the film consists of such a single phase with spinel-type structure, its composition can be considered as $\text{Fe}_{2.64}\text{Ge}_{0.36}\text{O}_4$.

3.2 Crystal structure of the reference sample $\text{Fe}_{2.7}\text{Ge}_{0.3}\text{O}_4$

At first, we started to refine the structural model with the random distribution of the Ge atoms both at the tetrahedral A and octahedral B sites with the chemical constraints. Converged occupation parameters for Ge at the A and B sites were 0.263(4) and 0.019, respectively. These results readily indicated the preferred distribution of Ge at the A site. The final positional and displacement parameters are presented in Table 2. The values of structural parameters of magnetite [19] are also summarized in Tables 1 and 2. The calculated interatomic distances are listed in Table 3 together with the reported values of Fe_2GeO_4 [20]. It should be added that the preferred residence of Ge at the A site was also observed in the case of brunogeierite $\text{Fe}_2^{2+}\text{GeO}_4$, from Tsumeb, Namibia [20].

The results of single crystal X-ray diffraction of $\text{Fe}_{2.7}\text{Ge}_{0.3}\text{O}_4$ suggest the mixed occupation of Ge and Fe atoms at the tetrahedral A site. Because the discrimination of Fe^{2+} and Fe^{3+} is difficult in the case of the ordinary single crystal X-ray diffraction, the present paper discusses their distribution based on the interatomic distances realized in the crystalline structure. In magnetite structure, the tetrahedral A sites are occupied by Fe^{3+} and the octahedral B sites are by Fe^{2+} and Fe^{3+} [19]. This information encourages us to simulate the tetrahedral A–O distance of the present sample using the distances of Ge–O(IV) and Fe^{3+} –O(IV) of brunogeierite and magnetite

together with the occupation parameter of 0.263. The calculated tetrahedral A–O distance of 0.1858 nm agreed well with the observed 0.18574(8) nm. This result supports the distribution of Fe^{3+} at the A site, leading the structural formulae of $[\text{Ge}_{0.263}\text{Fe}_{0.737}^{3+}]^{\text{IV}}[\text{Ge}_{0.038}\text{Fe}_{1.3}\text{Fe}_{0.662}^{3+}]^{\text{VI}}\text{O}_4$. Hereafter, the bulk $\text{Fe}_{2.7}\text{Ge}_{0.3}\text{O}_4$ was used as a reference sample of the Ge atoms coordinated by four oxygens.

3.3 XAFS analysis of $\text{Fe}_{2.64}\text{Ge}_{0.36}\text{O}_4$ thin films

The normalized Ge K XANES spectra for $\text{Fe}_{2.64}\text{Ge}_{0.36}\text{O}_4$ thin films and reference $\text{Fe}_{2.7}\text{Ge}_{0.3}\text{O}_4$ sample are shown in Figure 2. The energies of Ge K absorption edge for the thin film samples were almost equal to that of $\text{Fe}_{2.7}\text{Ge}_{0.3}\text{O}_4$. These results clearly indicate the fully oxidized state of Ge in the thin films. The XANES spectrum profile of the film annealed at 873 K was quite similar to that of $\text{Fe}_{2.7}\text{Ge}_{0.3}\text{O}_4$. This indicates that almost all Ge atoms in the film sample exist at the tetrahedral A site like in the reference $\text{Fe}_{2.7}\text{Ge}_{0.3}\text{O}_4$ sample. On the contrary, the XANES spectrum profiles of the as-synthesized and 573 K annealed films were similar to each other, but different from the profile of the 873 K annealed film. These results readily suggest that local atomic environment around Ge in the as-synthesized film is not similar to that coordinated tetrahedrally by four oxygens, and that the local structure is not changed by annealing at relatively low temperature.

The k^3 -weighted EXAFS spectra obtained from the X-ray absorption measurements at Ge K absorption edge for the $\text{Fe}_{2.64}\text{Ge}_{0.36}\text{O}_4$ thin film samples and reference $\text{Fe}_{2.7}\text{Ge}_{0.3}\text{O}_4$ are shown in Figure 3. The oscillation feature of the thin film sample annealed at 873 K was again quite similar to that of $\text{Fe}_{2.7}\text{Ge}_{0.3}\text{O}_4$. On the contrary, the k^3 -weighted EXAFS spectra of the film samples as-synthesized and annealed at 573 K showed different behavior together with rather broad oscillation nature at the wave vector region over 100 nm^{-1} , in particular. These results suggest the appearance of relatively complex structure with several additional interatomic correlations for the two film samples, which differ from that found in $\text{Fe}_{2.7}\text{Ge}_{0.3}\text{O}_4$ with the strong preference of tetrahedrally coordinated Ge (see Appendix).

The radial structure functions (RSFs) calculated from the k^3 -weighted EXAFS spectra in Figure 3 are shown in Figure 4. In the region of nearest neighboring Ge–O correlation of RSFs for the thin film samples as-synthesized and annealed at 573 K, a small shoulder **b** appeared at the farther side of Ge–O(IV) peak **a** corresponding to 0.1767 nm

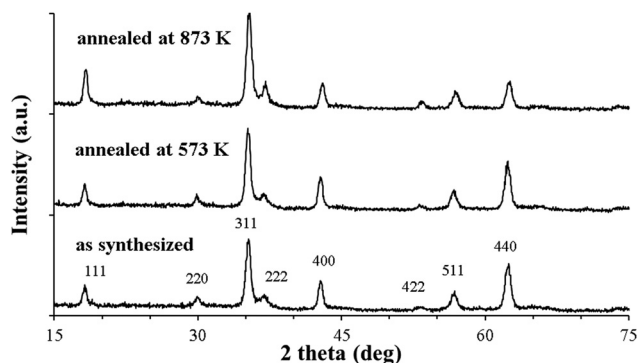


Figure 1: X-ray diffraction patterns of thin film samples measured at a fixed incidence angle of 3° .

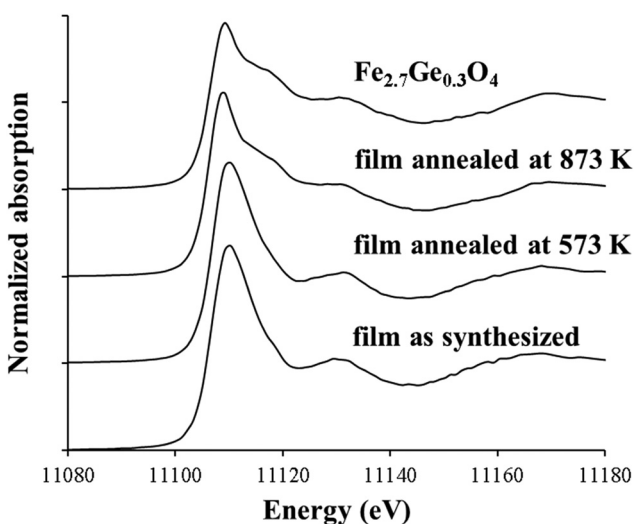
Table 2: Atomic coordinates and displacement parameters (10^{-2} nm²) for Fe_{2.7}Ge_{0.3}O₄

Chemical formula	Site	Occupancy	<i>x</i>	<i>y</i>	<i>z</i>	<i>U</i> ₁₁	<i>U</i> ₂₂	<i>U</i> ₃₃	<i>U</i> ₂₃	<i>U</i> ₁₃	<i>U</i> ₁₂
Fe _{2.7} Ge _{0.3} O ₄	A (8a)	Ge _{0.263(2)} Fe _{0.737}	1/8	1/8	1/8	0.00565(6)	<i>U</i> ₁₁	<i>U</i> ₁₁	0	<i>U</i> ₂₃	<i>U</i> ₂₃
	B (16d)	Ge _{0.019} Fe _{0.981}	1/2	1/2	1/2	0.00764(5)	<i>U</i> ₁₁	<i>U</i> ₁₁	0.00103(4)	<i>U</i> ₂₃	<i>U</i> ₂₃
	O (32e)	0	0.25258(6)	<i>x</i>	<i>x</i>	0.00903(10)	<i>U</i> ₁₁	<i>U</i> ₁₁	-0.00003 (17)	<i>U</i> ₂₃	<i>U</i> ₂₃

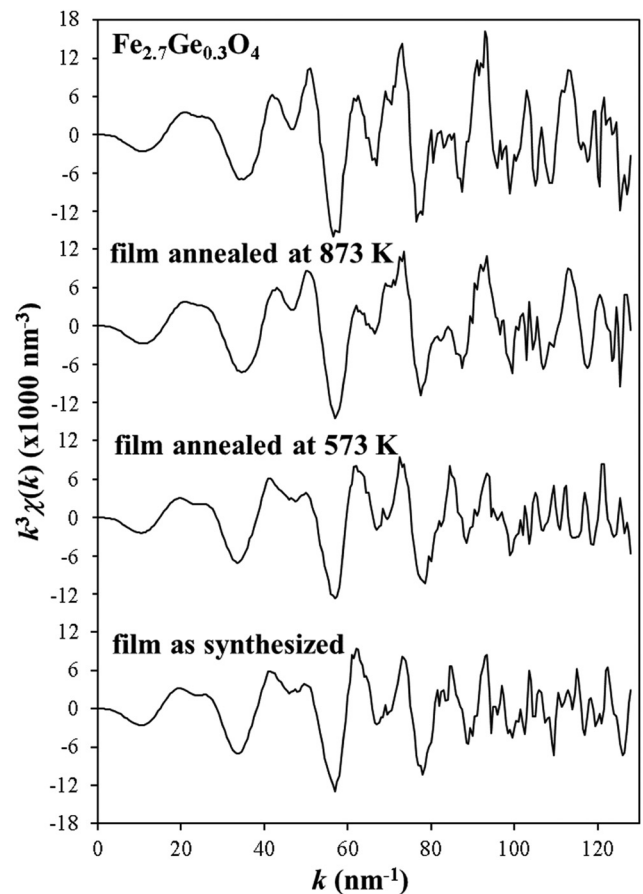
Table 3: Lattice parameter (nm) and interatomic distances (nm) of Fe_{2.7}Ge_{0.3}O₄, Fe₂GeO₄ (brunogeierite) [20], and Fe₃O₄ (magnetite) [19]

	Fe _{2.7} Ge _{0.3} O ₄ (this study)	Fe ₂ GeO ₄	Fe ₃ O ₄
Lattice parameter	0.84049(2)	0.84127(7)	0.8375(2)
A–O(vi)	Ge _{0.263} Fe _{0.737} : 0.18574(8)	Ge: 0.1771(2)	Fe ³⁺ : 0.1893(2)
B–O(vi)	Ge _{0.019} Fe _{0.981} : 0.20797(5)	Fe ²⁺ : 0.2132(2)	Fe _{0.5} ³⁺ Fe _{0.5} ²⁺ : 0.2049(2)

in distance determined by EXAFS analysis (see Table A1 in Appendix). In the region of cation–cation correlations, a shoulder **e** appeared at the closer side of A–B correlation peak **c** corresponding to 0.34845 nm in distance calculated from the lattice constant of Fe_{2.7}Ge_{0.3}O₄. It can be considered that Ge occupies partially the B site as well as the A site. The appearance of shoulder **b** and **e** can be explained respectively as B–O and B–B correlations, which do not exist in the interatomic correlations around Ge atoms occupying the A site. The measured magnetization for the as-synthesized Fe_{2.64}Ge_{0.36}O₄ thin film sample was 0.33 T. Although the magnetization value remained unchanged at 0.34 T after annealed at 573 K, it increased to 0.45 T when annealed at 873 K. The

**Figure 2:** Normalized XANES spectra measured at Ge *K* absorption edge for as-synthesized and annealed Fe_{2.64}Ge_{0.36}O₄ films with reference Fe_{2.7}Ge_{0.3}O₄.

ordering of Ge in the cation site distribution of magnetite structure is in good agreement with the annealing-induced magnetization increase behavior of the Fe_{2.64}Ge_{0.36}O₄ thin film.

**Figure 3:** *k*³-weighted EXAFS spectra measured at Ge *K* absorption edge for as-synthesized and annealed Fe_{2.64}Ge_{0.36}O₄ films with reference Fe_{2.7}Ge_{0.3}O₄.

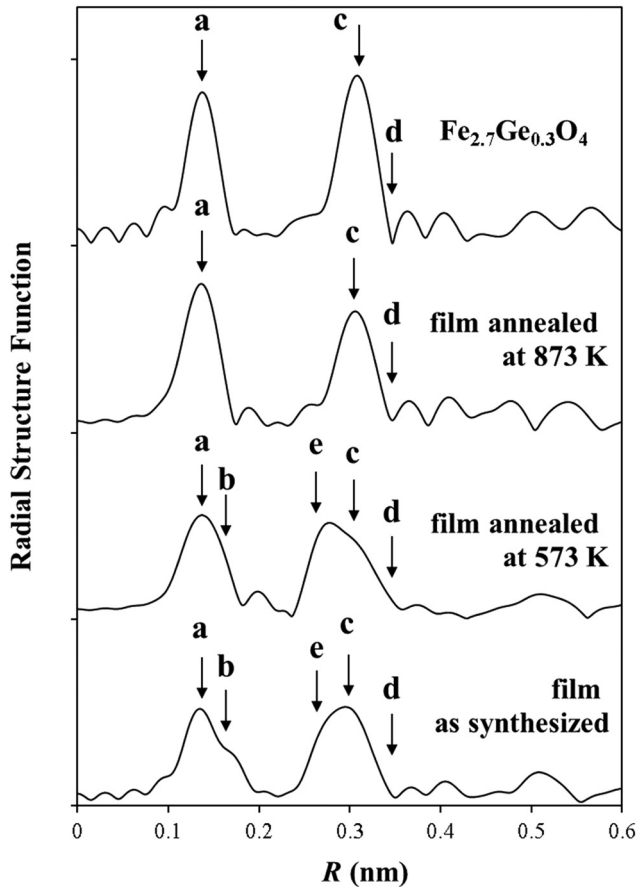


Figure 4: Radial structure functions obtained from the k^3 -weighted EXAFS spectra shown in Figure 2.

4 Summary

The local structure around Ge in $\text{Fe}_{2.64}\text{Ge}_{0.36}\text{O}_4$ thin films has been investigated by XAS. The structural analysis for measured EXAFS spectrum was made on the basis of the data obtained for a single crystal sample of 10 μm in diameter taken from the sintered $\text{Fe}_{2.7}\text{Ge}_{0.3}\text{O}_4$. The main results are summarized as follows:

- (1) Ge atoms showed the strong preference at the tetrahedral A site in the reference $\text{Fe}_{2.7}\text{Ge}_{0.3}\text{O}_4$.
- (2) In the $\text{Fe}_{2.64}\text{Ge}_{0.36}\text{O}_4$ thin film, distribution of the Ge atoms at the tetrahedral A and octahedral B sites was random for the as-synthesized film. The preferential A site occupation of the Ge atoms after annealing at 873 K was revealed by comparison of the EXAFS spectra from $\text{Fe}_{2.7}\text{Ge}_{0.3}\text{O}_4$ reference. It can be explained from comparison of EXAFS spectra with the results of local structure based on the single crystal structure analysis of $\text{Fe}_{2.7}\text{Ge}_{0.3}\text{O}_4$.

- (3) The ordering behavior of the Ge atoms in the site distribution by annealing corresponds well to the increase in magnetization of the thin film.

References

- [1] Aoshima, K.-I., and S. X. Wang. Fe_3O_4 and its magnetic tunneling junctions grown by ion beam deposition. *Journal of Applied Physics*, Vol. 93, No. 10, 2003, pp. 7954–7956.
- [2] Liu, H., E. Y. Jiang, and H. L. Bai. Large room-temperature spin-dependent tunneling magnetoresistance in polycrystalline Fe_3O_4 films. *Applied Physics Letters*, Vol. 83, No. 17, 2003, pp. 3531–3533.
- [3] Paramês, M. L., Z. Viskadourakis, M. S. Rogalski, J. Mariano, N. Popovici, J. Giepiantzakis, et al. Magnetic properties of Fe_3O_4 thin films grown on different substrates by laser ablation. *Applied Surface Science*, Vol. 253, No. 19, 2007, pp. 8201–8205.
- [4] D. M. Lind, S. D. Berry, G. Cherm, H. Mathias, and L. R. Testardi. Growth and structural characterization of Fe_3O_4 and NiO thin films and superlattices grown by oxygen-plasma-assisted molecular-beam epitaxy. *Physical Review B*, Vol. 45, No. 4, 1992, 1838–1850.
- [5] J. Cheng, G. E. Sterbinsky, and B. W. Wessels. Magnetic and magneto-optical properties of heteroepitaxial magnetite thin films. *Journal of Crystal Growth*, Vol. 310, No. 16, 2008, pp. 3730–3734.
- [6] D. T. Margulies, F. T. Parker, F. E. Spada, R. S. Goldman, J. Li, R. Sinclair, et al. Anomalous moment and anisotropy behavior in Fe_3O_4 films. *Physical Review B*, Vol. 53, No. 14, 1996, pp. 9175–9187.
- [7] Gong, G. Q., A. Gupta, G. Xiao, W. Qian, and V. P. Dravid. Magnetoresistance and magnetic properties of epitaxial magnetite thin films. *Physical Review B*, Vol. 56, No. 9, 1997, pp. 5096–5099.
- [8] Y. Peng, C. Park, and D. E. Laughlin. Fe_3O_4 thin films sputter deposited from iron oxide targets. *Journal of Applied Physics*, Vol. 93, No. 10, 2003, pp. 7957–7959.
- [9] Mauvernay, B., L. Presmanes, C. Bonningue, and Ph Tailhades. Nanocomposite $\text{Fe}_{1-x}\text{O}/\text{Fe}_3\text{O}_4$, $\text{Fe}/\text{Fe}_{1-x}\text{O}$ thin films prepared by RF sputtering and revealed by magnetic coupling effects. *Journal of Magnetism and Magnetic Materials*, Vol. 320, No. 1–2, 2008, pp. 58–62.
- [10] Abe, S., and S. Ohnuma. Magnetite thin films containing a small amount of Ge. *Applied Physics Express*, Vol. 1, No. 11, 2008, 111304.
- [11] Abe, S., D. H. Ping, S. Nakamura, M. Ohnuma, and S. Ohnuma. Metal-doped magnetite thin films. *Journal of Nanoscience and Nanotechnology*, Vol. 12, No. 6, 2012, pp. 5087–5090.
- [12] Abe, S. Ge-doped magnetite thin films with an enhanced resistance to oxidation. *Journal of Magnetism and Magnetic Materials*, Vol. 465, 2018, pp. 25–32.
- [13] Rigaku, O. D. *CrysAlis Pro*, Rigaku Oxford Diffraction Ltd, Yarnton, England, 2018.

- [14] International Tables for Crystallography Volume C. Dordrecht, Kluwer Academic Publishers, 1992.
- [15] Sheldrick, G. M. A short history of SHELX. *Acta Crystallographica Section A*, Vol. 64, Part 1, 2008, pp. 112–122.
- [16] Taguchi, T., J. Harada, K. Tohji, and K. Shinoda. An innovated laboratory XAFS apparatus. *Advances in X-ray Analysis*, Vol. 45, 2001, pp. 397–401.
- [17] Ravel, B., and M. Newville. ATHENA, ARTEMIS, HEPHAESTUS: Data analysis for X-ray absorption spectroscopy using IFEFFIT. *Journal of Synchrotron Radiation*, Vol. 12, Part 4, 2005, pp. 537–541.
- [18] Rehr, J. J., and R. C. Albers. Theoretical approaches to X-ray absorption fine structure. *Reviews of Modern Physics*, Vol. 72, No. 3, 2000, pp. 621–654.
- [19] Sasaki, S. Radial distribution of electron density in magnetite, Fe_3O_4 . *Acta Crystallographica B*, Vol. 53, Part 5, 1997, pp. 762–766.
- [20] Welch, M. D., M. A. Cooper, and F. C. Hawthorne. The crystal structure of brunogeierite, Fe_2GeO_4 spinel. *Mineralogical Magazine*, Vol. 65, No. 3, 2001, pp. 441–444.
- [21] Sickafus, K. E., J. M. Wills, and N. W. Grimes. Structure of spinel. *Journal of the American Ceramic Society*, Vol. 82, No. 12, 1999, pp. 3279–3292.

Appendix

Because the XAFS analysis is effective in determining the local atomic structure around a specific constituent, it is very interesting to discuss the local structural detail around Ge in $\text{Fe}_{2.7}\text{Ge}_{0.3}\text{O}_4$. Here, we show the results of FEFF simulation on the EXAFS spectrum of $\text{Fe}_{2.7}\text{Ge}_{0.3}\text{O}_4$ with strongly preferred distribution of Ge at the tetrahedral A site. The coordination correlations around the Ge atoms such as Ge–O(IV) and cation–cation correlations of A–B and A–A are required in FEFF simulation [21]. The value of Ge–O(IV) distance was determined by the least-squares fitting though the values of cation–cation interatomic distances were fixed to those determined inevitably from the lattice constant obtained by single crystal structure analysis. Considering the occupancy ratio of Ge:Fe = 0.263:0.737 and 0.019:0.981 for A and B sites shown in Table 2, the values of coordination numbers for cations

around a Ge at tetrahedral A site can be assigned to 1 Ge and 3 Fe of 4 coordinated cations at A site and all Fe of 12 coordinated cations at B site. The resultant parameters are summarized in Table A1 and the calculated k^3 -weighted EXAFS spectrum including all correlations and the spectra corresponding to contribution of each correlation are shown in the left side of Figure A1 with the RSFs obtained by Fourier transformation of the EXAFS spectra in the wave number region from 28 to 128 nm^{-1} on the right side. For the region of cation–cation correlations in the RSF, calculated profile using the structure parameter values for A–B correlation **c** and A–A correlation **d** obtained from the lattice constant was in good agreement with the observed one. The nearest neighboring Ge–O (correlation **a**) distance (0.1767 nm) obtained by the least-squares fitting showed good agreement with the Ge–O(IV) distance realized in brunogeierite $\text{Fe}_2^+\text{GeO}_4$.

Table A1: Resultant values of the interatomic distance from structure analysis of Ge K-EXAFS for the crystalline $\text{Fe}_{2.7}\text{Ge}_{0.3}\text{O}_4$ sample

Pair	<i>N</i>	<i>r</i> (nm)	ΔE_0 (eV)	σ^2 (nm ²)
Ge–O	4	0.1767	6.682	0.000032
Ge–Fe(B)	12	0.34845	6.261	0.000050
Ge–Fe(A)	3	0.36395	7.984	0.000057
Ge–Ge(A)	1	0.36395	6.261	0.000027

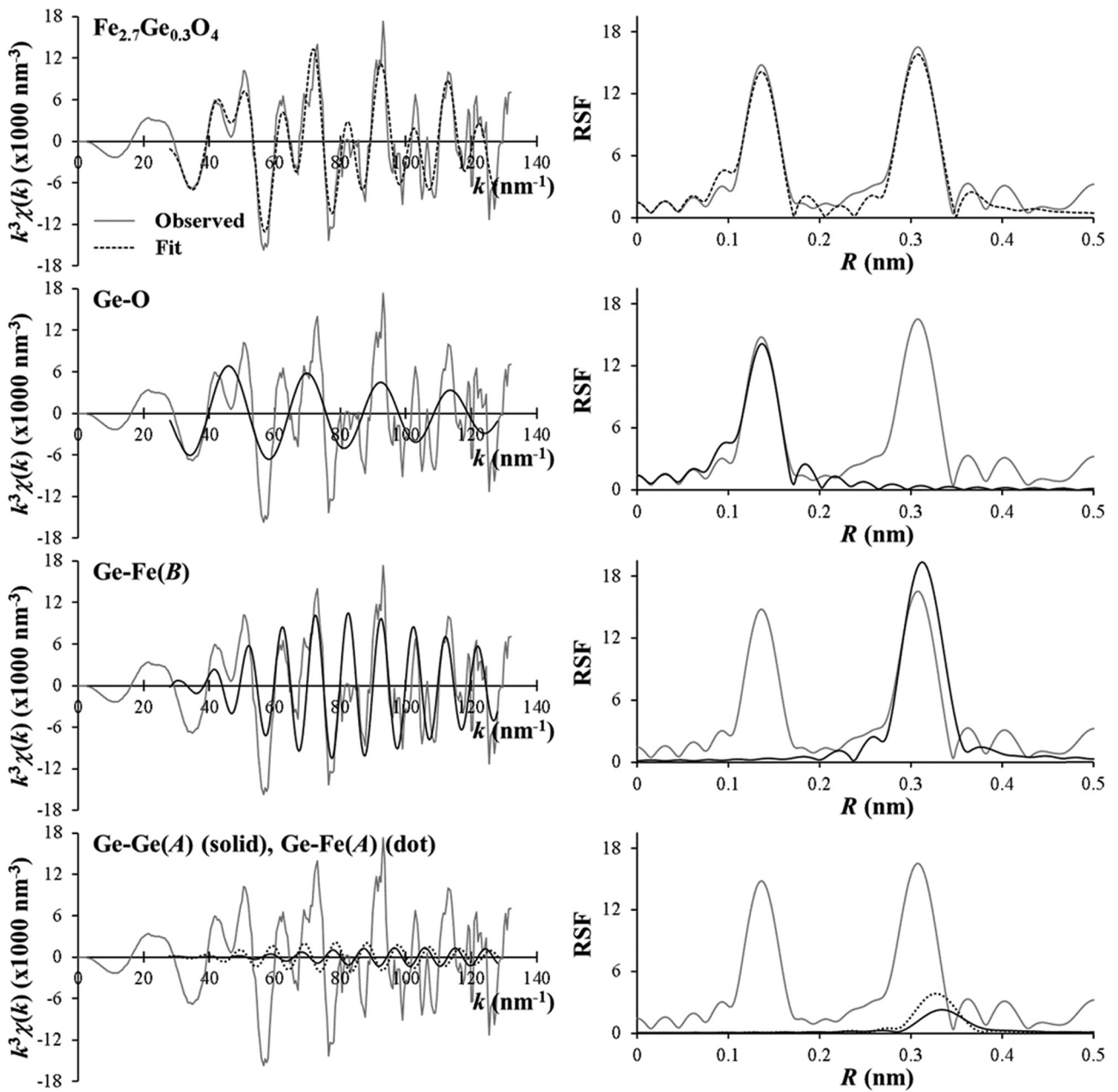


Figure A1: The calculated EXAFS spectrum and RSF for the reference $\text{Fe}_{2.7}\text{Ge}_{0.3}\text{O}_4$ based on a structure model that all Ge atoms are considered to distribute the tetrahedral A site. The top two figures show the total spectrum and RSF including the four correlations of Ge occupying the A site. The three paired figures below show each correlation of O, Fe in the B site, and Fe and Ge in the A site around Ge, respectively.